

Exploring the Mechanism of Electron Transfer between DNA and a Ternary Copper Complex

Debarati Dey,[†] Nikhil R. Pramanik,[‡] and Samita Basu^{*,§}

Department of Chemistry & Environment, Heritage Institute of Technology, Chowbaga Road, Anandapur, P.O. East Kolkata Township, Kolkata 700107, India; Department of Chemistry, Chandernagar Government College, Chandernagar, India; and Chemical Sciences Division, Saha Institute of Nuclear Physics, 1/AF, Bidhannagar, Kolkata 700064, India

Received: December 8, 2008; Revised Manuscript Received: March 28, 2009

Photoinduced intramolecular electron transfer occurs in the triplet state within the complex [Htyr-Cu-phen]⁺ (Htyr = L-tyrosinato; phen = 1,10-phenanthroline) from tyrosine to phenanthroline. For this linked donor–acceptor system, a prominent magnetic field effect (MFE) is observed for the triplet-born radicals. The competitive binding study in the presence of ethidium bromide suggests that the complex interacts with calf thymus DNA (CT DNA) through partial intercalation. The photoexcited copper complex can oxidize DNA in a deoxygenated environment. Though the oxidation of tyrosine is thermodynamically more favorable than the oxidation of guanine, the primary electron transfer occurs from the DNA base to the phen ligand. A prominent MFE is observed for this noncovalently bound triplet-born guanine radical and phen radical anion. The process of partial intercalation of the copper complex within DNA is responsible for this rare observation.

Introduction

Recent research has focused on electron transfer reactions between molecules bound to macromolecular assemblies such as polymer, micelles, and biomolecules.^{1–3} In such systems, besides the covalent bonding, the noncovalent weak interactions such as hydrogen bonding, electrostatic attractions, and aromatic ring stacking play vital roles.^{4,5} Moreover, in comparison to supramolecular systems, it is important to understand how the host medium manipulates the reactivity of the guest molecules. In this paper, we report about the intramolecular photoinduced electron transfer phenomenon within a copper complex and then compare and contrast how the reaction is influenced by the presence of CT DNA.

Among the four amino acids with an aromatic side chain—phenylalanine, tyrosine, tryptophan, and histidine—phenylalanine contributes mainly to the stabilization of proteins through hydrophobic interactions whereas tryptophan has an electron-rich indole ring which has an excellent π electron donating property. Histidine and tyrosine have effective metal binding sites. The presence of the tyrosine molecule in the active site of enzymes such as galactose oxidase and the subsequent formation of tyrosine radicals is attracting much attention.^{6,7} Further, aromatic amino acid residues in particular have been shown to engage in stacking interactions with nucleic acid bases and could represent a possible target for oxidative damage through radical migration.^{8–11} Hence, the solution studies of ternary metal complexes comprising aromatic amino acids, especially tyrosine, and as a second ligand which contains an aromatic ring such as 2,2'-bipyridine or 1,10-phenanthroline, are important to understand the electron transfer reactions between the amino acid and heterocyclic molecules.

In this paper, we report about the mode of interaction of a ternary copper complex [Htyr-Cu-phen]ClO₄ (**1**) (phen = 1,10-phenanthroline; Htyr = L-tyrosinato) with DNA and then study how the macromolecule affects the photoinduced electron transfer (PET) reactions of the complex. The occurrence of PET reactions could be verified by applying an external small magnetic field (MF).

The PET reactions produce initially geminate radical ion pairs (RIPs) that contain two spin-correlated free electrons.^{12–16} Magnetic field effect (MFE) is basically interplay between spin dynamics and diffusion dynamics. By diffusion the RIPs can separate to an optimum distance where the exchange interaction (J) becomes negligible. In this situation, the electron–nuclear hyperfine coupling induces efficient mixing between the triplet (T_{\pm}, T_0) and the singlet (S) states. The application of an external MF of the order of hyperfine interaction removes the degeneracy of the triplet states and reduces intersystem crossing (ISC), thus resulting in an increase in the population of the initial spin state. This is reflected from the increase in absorbance and decrease in decay rate constant of the transients produced. Thus, MFE importantly serves to identify the initial electronic spin state of the RIPs. Again, the MFE is very much sensitive to the distance between the participating radical ions because the hyperfine induced spin flipping depends on J , which in turn has exponential distance dependence. When the RIPs are in contact, the S – T splitting caused by J is much stronger than the hyperfine coupling energies so that spin evolution cannot occur by this mechanism. On the other hand, at a distance where J is sufficiently small S – T conversion becomes facile. However, if the separation between the two radicals is too far, the geminate characteristics get lost and consequently MFE cannot be observed. Therefore, an optimum separation between the RIPs is required so that both spin flipping and recombination are feasible. Generally, MFE experiments on the triplet born transients involve micellar media^{17,18} or highly viscous solvents^{19–21} at low temperature or long-chain biradicals^{22,23} to reduce fast escape thus retaining the spin correlation between the partners

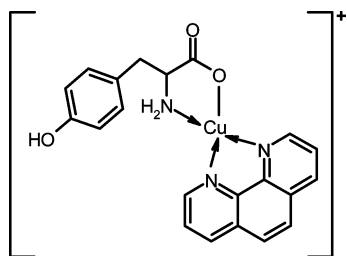
* Corresponding author. E-mail: samita.basu@saha.ac.in. Tel.: +91-33-2337-5345. Fax: +91-33-2337-4637.

[†] Heritage Institute of Technology.

[‡] Chandernagar Government College.

[§] Saha Institute of Nuclear Physics.

CHART 1: Chemical Structure of Complex (1)



of the geminate RIP. However, there are few examples found in the literature where MFE has been detected in homogeneous medium by transient absorption of the triplets and the radical ions.^{24–33} Interestingly, we have found prominent MFE for the triplet born radicals not only in the case of intramolecular electron transfer but also for the intermolecular electron transfer between DNA and [Htyr-Cu-phen]⁺ even in homogeneous aqueous medium. The observation of MFE for the intraligand charge transfer within **1** is very much familiar in literature just like a linked system.¹⁶ However, the occurrence of MFE for noncovalently linked triplet born radicals in homogeneous medium is rather rare. The process of partial intercalation of the complex **1** within DNA might be responsible for the observation of MFE in homogeneous medium.

Experimental Section

Materials. Tris buffer was obtained from Spectrochem. Highly polymerized double-stranded calf thymus DNA (CT DNA) was purchased from Sisco Research Laboratory, India, and used as received. Ethidium bromide (EtBr) was purchased from Merck, Germany. 1,10-Phenanthroline and L-tyrosine were purchased from Sigma. The copper complex [Htyr-Cu-phen](ClO₄)·2.5H₂O (**1**) (Chart 1) was prepared in the laboratory by adopting the procedure described in ref 34. It was purified by repeated crystallization. Anal. Calcd for Cu(phen)(Htyr)-(ClO₄)·2.5H₂O: C, 44.44; H, 3.88; N, 7.41. Found: C, 44.41; H, 2.62; N, 8.67. Water was triply distilled.

Methods and Instrumentation

Studies Using Absorption Spectroscopy. UV–vis absorption spectra were recorded on a Shimadzu UNICAM-UV-500 absorption spectrophotometer. A pair of 1 × 1 cm path length quartz cuvettes was used for absorption experiments. All the experiments involving the interaction of the copper complex with DNA were carried out in 50 mM Tris HCl buffer and 5 mM NaCl at pH 7.4. After the DNA fibers were dissolved in the buffer their purity was checked from the absorbance ratio A_{260}/A_{280} . The ratio was found to remain within 1.8–1.9. Therefore, further deproteinization of DNA solution was not needed. The concentration of CT DNA was determined from absorption intensity at 260 nm with the known molar extinction coefficient of 6600 cm² mol^{−1} at 260 nm.

Absorption experiments were performed by maintaining the metal complex concentration as constant while varying the CT DNA concentration. As both **1** and DNA have absorption in the same region, during measurement of the absorption spectra equal quantity of CT DNA has been added to both the complex solution and in the reference solution to eliminate the absorbance of DNA itself and to monitor the changes of the complex **1** in the presence of DNA.

Competitive Binding Study. Competitive binding of the complex in the presence of EtBr with CT DNA has been studied

using fluorescence spectroscopy. EtBr does not show any emission in buffer medium due to fluorescence quenching of the free EtBr by solvent molecules.³⁵ In the presence of CT DNA it shows enhanced emission intensity due to insertion of the molecule within the hydrophobic region of the DNA base pairs. A competitive binding of the complex **1** to CT DNA in the presence of EtBr possibly causes displacement of the intercalated EtBr molecule from DNA backbone. As a result, the emission intensity of EtBr reduces on addition of the complex. During this study, EtBr bound CT DNA solution in buffer was treated with an increasing concentration of complex. The fluorescence intensity at 600 nm ($\lambda_{\text{ex}} = 512$ nm) of DNA-bound EtBr has been plotted against the complex concentration.

Preparation of Reverse Micelles. AOT (sodium bis(2-ethylhexyl)sulfosuccinate) reverse micelles were prepared in heptane (HP).³⁶ The complex and DNA was mixed in buffer and the desired amount of this buffer was added for W_0 variation ($W_0 = [\text{H}_2\text{O}]/\text{molar concentration of the reverse micelle}$) as described by Imre and Luisi.³⁷ The final concentration of the complex was 40 μM . The concentration of the surfactant was 0.2 M.

Transient Absorption Measurement. The transient absorption spectra were measured by using a nanosecond flash photolysis setup (Applied Photophysics) having a Nd:YAG laser (DCR-11, Spectra Physics) described elsewhere.³⁸ The sample was excited by 266 nm laser light with ~ 8 ns fwhm. Transients were monitored through absorption of light from a pulsed Xe lamp (250 W). The photomultiplier (IP28) output was fed into a Tektronix oscilloscope (TDS 3054B, 500 MHz, 5 Gs/s), and the data were transferred to a computer using the TekVISA software. MFE on the transient absorption spectra was studied by passing dc through a pair of electromagnetic coils placed inside the sample chamber. The strength of MF can be varied from 0.0 to 0.08 T. The software Origin 5.0 was used for curve fitting. All the samples were deaerated by passing pure argon gas for 20 min prior to the experiment. No degradation of the samples was observed during the experiment.

In general, cupric complexes do not exhibit any intense charge transfer or a sufficiently intense d–d band suitable for monitoring their interaction with DNA. So the ligand-based intense ($\pi \rightarrow \pi^*$) absorption band is used to monitor the interaction of **1** with CT DNA. Both complex **1** and DNA have significant absorbance at 266 nm wavelength. Therefore, when we excite a mixture of **1** and DNA with 266 nm laser light, there is the possibility of excitation of both **1** and DNA. However, the extinction coefficient of DNA at 266 nm is ~ 6600 mol^{−1} cm², whereas that of **1** is $\sim 44\,814$ mol^{−1} cm². Therefore, when a mixture of **1** and DNA is excited by 266 nm laser light, the probability of excitation of DNA is very much lower compared to **1**.

Results and Discussion

Interaction of Complex (1) with Calf Thymus DNA. The ternary copper complex **1** exhibits two peaks in the UV region at 218 and 269 nm. Beside the UV peaks it shows a d–d band at 606 nm. As the extinction coefficient of the d–d band is much lower compared to the UV bands we have focused on the UV bands for DNA binding studies. Upon addition of calf thymus DNA considerable amount of hypochromicity has been observed with a slight red shift of the UV bands. In general, a compound bound to DNA through intercalation usually results in hypochromism accompanied by a red shift of the absorption band due to strong stacking interaction between aromatic chromophore of the compound and the base pairs of the DNA.

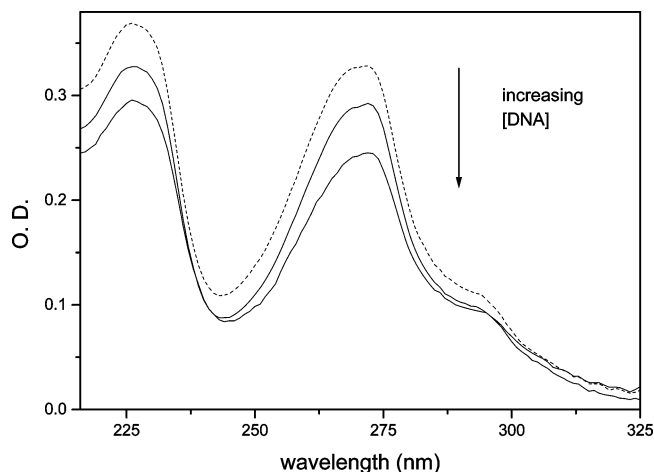


Figure 1. Steady-state absorption spectra of complex **1** with different concentrations of DNA: 0 μM (---), 25 μM , and 50 μM .

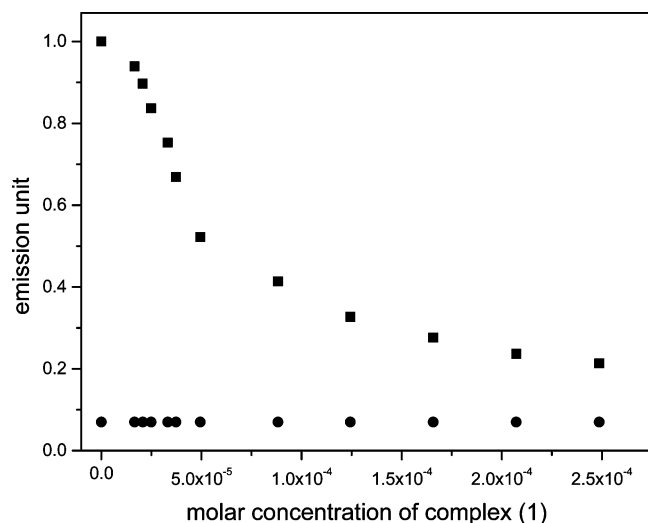


Figure 2. Quenching of the emission intensity of CT DNA bound EtBr (4.5 μM) (■) and free EtBr (●) at different complex **1** concentrations ($\lambda_{\text{ex}} = 512 \text{ nm}$). The concentration of CT DNA was 100 μM .

Figure 1 shows the decrease in absorbance of the two UV bands with increasing concentration of DNA. This suggests that the copper(II) complex interacts with CT DNA probably through intercalation.

Competitive Binding of Complex (1) with CT DNA in the Presence of EtBr. The binding of **1** to CT DNA in the presence of known intercalator EtBr has been studied by fluorescence spectroscopy using emission intensity of EtBr. The concentration of EtBr (4.5 μM) with respect to DNA (100 μM) is such that all the EtBr are intercalating within the double-stranded DNA and there is no EtBr remaining free in the solution. On addition of complex **1**, the fluorescence intensity of DNA-bound EtBr decreases as shown in Figure 2. This suggests that the complex **1** can displace the inserted EtBr from CT DNA, although a much higher concentration of complex **1** is required than that of EtBr. There may be another possible explanation that complex **1** first binds to DNA in the vacant intercalating sites and induces some structural changes on DNA, resulting in a change of local environment around the intercalated EtBr, which renders the intercalated EtBr exposed to aqueous environment from the hydrophobic environment of DNA. Whichever the phenomena, it is clear that complex **1** interacts with DNA and the mode interaction might be partial intercalation.

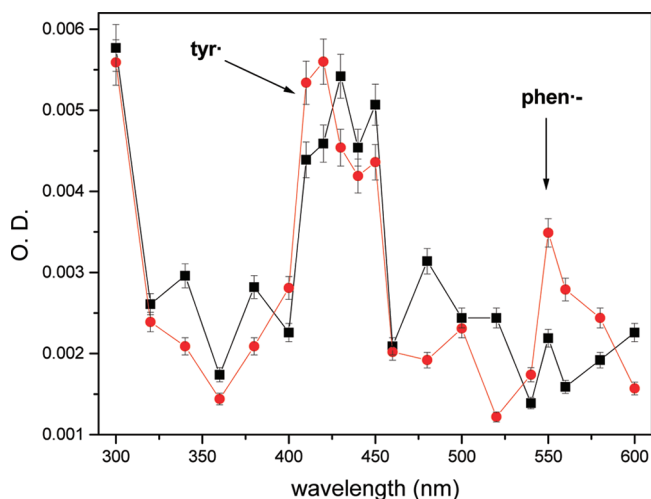


Figure 3. Transient absorption spectra of complex **1** (40 μM) in buffer in the absence (■) and presence (●) (red) of 0.08 T MF at 0.6 μs after the laser flash.

TABLE 1: Decay Rate Constant of Tyr \cdot Radical in the Presence and Absence of MF

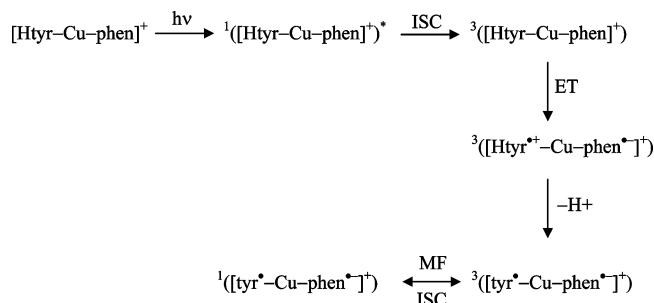
system	medium	magnetic field (T)	$k_f \times 10^{-5}$ (s^{-1})	Y^b
complex 1	buffer ^c	0.00	3.28	1.00 ^a
		0.08	1.95	1.33
complex 1 –DNA	buffer ^d	0.00	1.22	1.00 ^a
		0.08	0.67	1.64
	AOT reverse micelle ^e	0.00	5.73	1.00 ^a
		0.08	5.04	1.21

^a Arbitrarily taken. ^b Escape yield after 5 μs . ^c At 410 nm. ^d At 390 nm. ^e At 380 nm.

MFE for Intramolecular Electron Transfer. The triplet–triplet absorption of **1** ($4 \times 10^{-5} \text{ M}$) shows a maximum around 430 nm (Figure 3, black curve). Besides this a shoulder appears at 410 nm and a small peak appears at 550 nm. Previously, it was shown that the bis(phenanthroline) analogue $[\text{Cu}(\text{phen})_2]^{2+}$ shows triplet–triplet peak at 440 nm.⁴¹ In the presence of an external MF, a prominent MFE is observed at 410 and 550 nm (Figure 3, red curve). It is well-known from the literature that tyrosyl radical tyr^\cdot appears at 410 nm^{39,40} and phenanthroline radical anion appears at 550 nm.⁴¹ This implies that on photoexcitation an intramolecular electron transfer occurs within the complex from tyrosine to the phenanthroline moiety in the triplet state. As both tyrosine and phen ligands are attached to the Cu(II) center by covalent and coordinate covalent bonding, so after electron transfer the radical ions produced cannot go far apart from each other. Thus, the geminate characteristics of the radical ions are preserved for longer time. If the exchange interactions between the two free electrons of the geminate RIP become negligible, then maximum ISC occurs between the triplet and the singlet state. Application of an external MF of the order of HFI suppresses the ISC by introducing Zeeman splitting in the triplet sublevels, which in turn increases the yield of the free ions in the initial spin state. Thus, in this case MFE is found for the triplet born radicals that is very similar to that of linked donor and acceptor system. The decay rate constant of tyr^\cdot radical in the presence and absence of MF is given in Table 1.

The decay of the RIPs is expected to be biexponential. The change in absorbance $A(t)$ with time follows the expression $A(t) = I_f \exp(-k_f t) + I_s \exp(-k_s t)$, where k_f and k_s are the rate constants for the fast and slow components of the decay profiles,

SCHEME 1: Intramolecular Photoinduced Electron Transfer



respectively.⁴² The fast component corresponds to the decay of geminate RIPs and the slower one corresponds to the reaction of the escaped radicals. The k_f values obtained by biexponential fitting from the decay profiles in the absence and in the presence of MF are given in Table 1. The relative escape yields after 5 μs (Y) are also calculated (Table 1). It is observed that, on application of an external magnetic field, the decay rate decreases and correspondingly the escape yield increases. This also implies that the RIPs are generated in the triplet spin state. On application of an external magnetic field, the ISC of the triplet RIPs to the singlet RIPs is decreased and consequently the decay rates become slower and escape yield gets enhanced.

On photoexcitation initially ${}^1([\text{Htyr-Cu-phen}]^+)^*$ is formed, which then undergoes a rapid ISC to form ${}^3([\text{Htyr-Cu-phen}]^+)^*$. Then intramolecular electron transfer occurs from phenol moiety of Htyr to phen leading to corresponding radical ions. After electron transfer the tyrosyl radical cation Htyr^{++} can lose a proton to give the corresponding radical tyr^* . The mechanism of the reaction is shown in Scheme 1.

MFE for Intermolecular Electron Transfer between CT DNA and (1) in Buffer and in AOT Reverse Micelles. Figure 4 shows the transient absorption spectra of pure complex **1** and **1** in the presence of CT DNA in buffer medium at 0.6 μs after laser flash. In the presence of DNA a substantial quenching is observed for the triplet-triplet absorption of complex **1** DNA with rising peak at 380 and 510 nm, while the peak at 550 nm increases slightly. Therefore, electron transfer might occur between photoexcited complex and DNA. The peak around 380 and 510 nm is due to the formation of DNA radical cation,^{43,44}

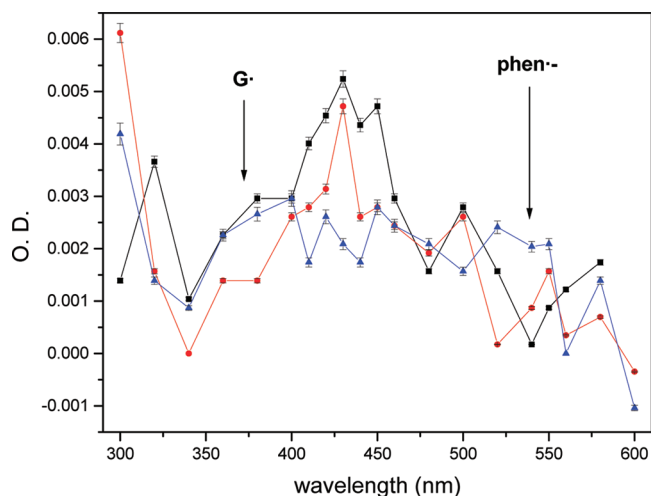


Figure 4. Transient absorption spectra of the complex **1** (40 μM) at different DNA concentrations 0.0 μM (■) (black), 40 μM (●) (red), and 120 μM (▲) (blue) in buffer at 0.6 μs after the laser flash.

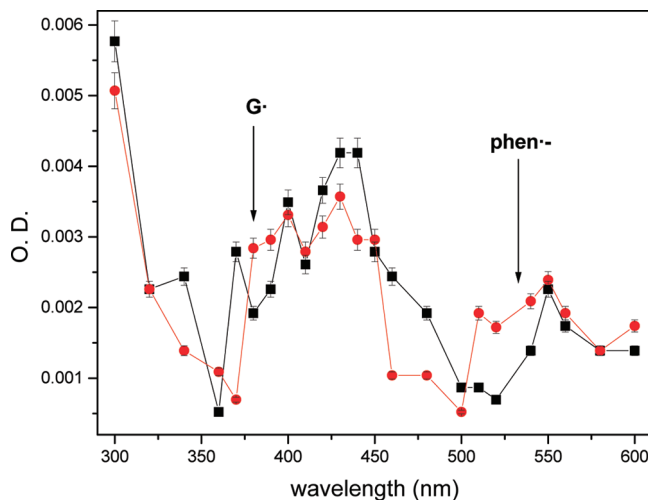
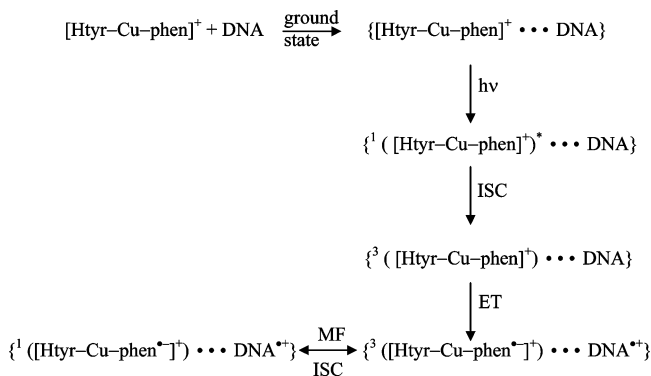


Figure 5. Transient absorption spectra of the complex **1** (40 μM)-DNA (80 μM) in buffer in the absence (■) and presence (●) of 0.08 T MF at a delay of 0.6 μs after the laser flash.

DNA⁺⁺. As we know that the guanine base is the most easily oxidizable component of DNA, so the DNA radical cation might be of guanine radical cation G^{++} that readily deprotonates to guanine radical. This hump becomes much more prominent with increasing concentration of DNA. The quenching phenomenon of **1** in the presence of DNA also proves that in the presence of **1**, DNA itself may not absorb the laser light. In the presence of an external MF a prominent MFE is also observed for both the guanine radical and phenanthroline radical anion as shown in Figure 5. The fast component of the biexponential decay of the RIPs and their escape yields after 5 μs are given in Table 1.

It was shown in the previous work in our laboratory⁴¹ that partial intercalators might show prominent MFE in homogeneous buffer medium for the triplet born radicals during electron transfer reaction with DNA. Due to imperfect intercalation, i.e., partial insertion of a part of a large molecule within DNA base pairs, the optimum distance of separation between the donor and acceptor molecule is maintained with negligible exchange interaction favoring the occurrence of the MFE for triplet-born radicals even in homogeneous buffer medium. In our present case, the complex **1** can displace a perfect intercalator like EtBr. The crystal structure of **1**³⁴ shows that it has distorted square pyramidal environment around the Cu(II) ion. The four equatorial sites are occupied by a bidentate tyrosinato ligand through carboxylate oxygen and amino nitrogen atom and a bidentate phen ligand. The oxygen atom of a water molecule occupies the axial position. However, the perfect intercalation of complex **1** within DNA is not feasible due to the nonplanar structure of complex **1**.

One relevant question may arise in this context. A close observation of the reduction potentials of guanine and tyrosine reveals that reduction potential of guanosine radical is 1.29 V, which is considerably higher than that of tyrosine (0.9 V). Therefore, an electron transfer from tyrosine to guanosine radical is thermodynamically feasible.⁴⁵ Despite the favorable thermodynamics, electron is not directly transferred from tyrosine to phenanthroline in the presence of DNA. The appearance of MFE in case of guanine radical suggests that electron transfer occurs through the intermediacy of the guanine radical. It was earlier reported by Barton et al.⁴⁶ that, though the oxidation of tyrosine is more favorable than guanine, in spite of that DNA damage by guanine oxidation is observed even in the presence of tyrosine. They have suggested that the guanine oxidation is a

SCHEME 2: Intermolecular Photoinduced Electron Transfer

kinetically faster process and its decay starts simultaneously with the rise of the thermodynamically favorable tyrosyl radical. We have found a prominent MFE for the guanine radicals in the time scale of 0.6 μs . This further supports the fact that the electron first goes from the DNA base instead of tyrosine. In the presence of DNA, MFE for the tyrosyl radical is not prominent. This is due to the reason that when the repair of guanine radical produces thermodynamically favorable tyrosyl radical the geminate characteristics of the RIPs is lost. The mechanism of reaction is given in Scheme 2.

In AOT reverse micelles the intermolecular electron transfer phenomenon is also observed. Reverse micelles consist of a homogeneous thermodynamically stable solution of nanodroplets of water surrounded by a surfactant monolayer and dispersed in an organic solvent. These water nanodroplets are used as confined system. For a given concentration of AOT, the size of the entrapped water pool and hence that of the reverse micelle depends on the ratio between water and AOT molecules ($W_0 = [\text{H}_2\text{O}]/[\text{AOT}]$). The water pool size is given by $2W_0$.

Figure 6 shows the transient absorption spectra of the complex 1–DNA system in the presence and absence of MF in AOT reverse micelles. A prominent MFE is observed for the guanine radical at 385 nm. The decay constants of the fast component and the escape yields after 5 μs in absence and presence of MF are given in Table 1. It is evident from the rate constant (k_f) and the escape yield (Y) that the MFE is not very much strong

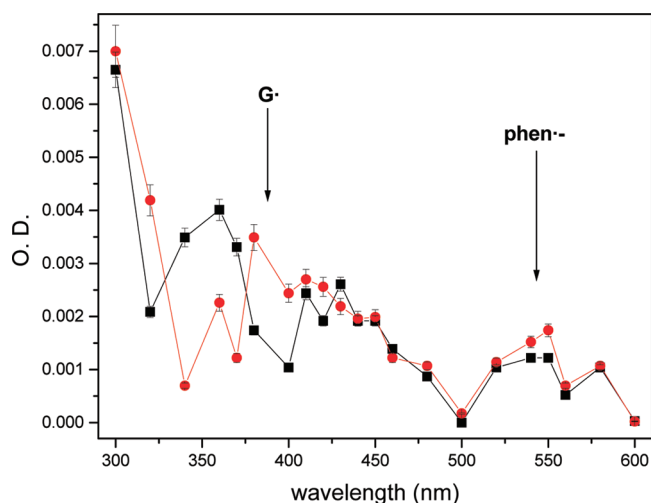


Figure 6. Transient absorption spectra of the complex 1 (40 μM)–DNA (80 μM) in AOT reverse micelle in the absence (■) and presence (●) (red) of 0.08 T MF at a delay of 0.6 μs after the laser flash.

in AOT reverse micelle as that in buffer. We have found maximum MFE at $W_0 = 10$. Above and below this W_0 value the MFE dies out rapidly. As mentioned earlier, the observation of MFE involves diffusion, spin flipping, and geminate recombination. When the participating radicals are close to each other (small W_0), the exchange interaction, J , will hinder spin conversion and at a large distance of separation (large W_0), spin correlation will be lost. So MFE requires an optimum separation between the participating RIP that is attained at an intermediate W_0 . This optimum W_0 may not be the same for all the acceptor–donor systems studied. However, the observed MFE in AOT reverse micelle is not very strong, as expected in confined system, compared to homogeneous medium. The reason behind is that the monovalent cation of the complex is hydrophobic in nature. It readily dissolves into organic medium, e.g., in heptane, than in water. Thus, when we add the complex, dissolving it in water, into AOT reverse micelles in heptane, the complex becomes partitioned between water and heptane. Thus, the effective concentration of the complex in the water pool decreases on the one hand and on the other hand the distance between the donor and acceptor molecules increases, which lead to the decrease of the extent of MFE in AOT.

Conclusion

A prominent MFE is observed for the intramolecular electron transfer within complex 1, which is very similar to that of linked donor–acceptor system. In the presence of DNA an intermolecular electron transfer reaction takes place between DNA and complex 1 either in homogeneous buffer medium or in AOT reverse micellar medium. In the case of intermolecular electron transfer, although the complex 1 is not covalently linked with DNA, they behave like a linked system due to partial intercalation. Quenching of DNA bound EtBr fluorescence by $[\text{Htyr-Cu-phen}]^+$ suggests that the copper complex can displace EtBr from DNA backbone. The driving force for intercalation is the electrostatic force of attraction between the positively charged complex and negatively charged DNA, and the hydrophobic interaction between phenanthroline ring and DNA base pairs. But due to the nonplanar structure of complex 1, perfect intercalation between DNA base pairs is not possible. Observation of a prominent MFE for the guanine radical in the presence of DNA suggests that electron transfer first occurs from the guanine base, instead of tyrosine, to phen moiety though electron transfer from tyrosine is thermodynamically more favorable. The occurrence of partial intercalation of complex 1 within DNA helps in maintaining the proper distance between the RIPs, generated through PET, so that spin correlation can occur between them. This results in the observation of MFE in homogeneous aqueous medium. In a confined system like AOT reverse micelles, the MFE is expected to be larger compared to that in aqueous medium, but in this case the partitioning of complex 1 in organic medium increases the interradical distance that breaks the spin correlation of geminate RIPs, and thus MFE gets reduced.

Acknowledgment. We sincerely thank Mrs. Chitra Raha of SINP for her kind assistance and technical support. We also thank Prof S. S. Mondal of the University College of Science and Technology, Mr. Manas Kumar Sarangi of SINP, and Ms. Doyel Das of IACS, India, for their cooperation.

References and Notes

- (1) Jones, W. E.; Baxter, S. M.; Strouse, G. F.; Meyer, T. J. *J. Am. Chem. Soc.* **1993**, *115*, 7363.

- (2) Turro, N. J.; Barton, J. K.; Tomalia, D. A. *Acc. Chem. Res.* **1991**, *11*, 332.
- (3) Boxer, S. G. *Annu. Rev. Biophys. Biophys. Chem.* **1990**, *19*, 267.
- (4) Christianson, D. W.; Lipscomb, W. N. *Acc. Chem. Res.* **1989**, *22*, 62.
- (5) Amit, A. G.; Mariuzza, R. A.; Phillips, S. E. V.; Poljak, R. J. *Science* **1986**, *233*, 747.
- (6) Ito, N.; Phillips, S. E. V.; Stevens, C.; Ogel, Z. B.; McPherson, M. J.; Keen, J. N.; Yadav, K. D. S.; Knowles, P. F. *Nature* **1991**, *350*, 87.
- (7) Ito, N.; Phillips, S. E. V.; Stevens, C.; Yadav, K. D. S.; Knowles, P. F. *J. Mol. Biol.* **1994**, *238*, 794.
- (8) King, G. C.; Coleman, J. E. *Biochemistry* **1987**, *26*, 2929.
- (9) Suzuki, M. *Nature* **1990**, *344*, 562.
- (10) Kim, Y.; Geiger, J. H.; Hahn, S.; Sigler, P. B. *Nature* **1993**, *365*, 512.
- (11) Kim, J. L.; Nikolov, D. B.; Burley, S. K. *Nature* **1993**, *365*, 520.
- (12) Steiner, U. E.; Ulrich, T. *Chem. Rev.* **1989**, *89*, 51.
- (13) Bhattacharya, K.; Chowdhury, M. *Chem. Rev.* **1993**, *93*, 507.
- (14) *Dynamic spin chemistry magnetic controls and spin dynamics of chemical reactions*; Nagakura, S., Hayashi, H., Azumi, T., Eds.; Kodansha Ltd./John Wiley & Sons Inc.: Tokyo/New York, 1998.
- (15) Gould, I. R.; Turro, N. J.; Zimmt, M. B. *Adv. Phys. Org. Chem.* **1984**, *20*, 1.
- (16) Tanimoto, Y.; Fujiwara, Y. In *Handbook of Photochemistry and Photobiology Vol. 1: Inorganic Chemistry*; Nalwa, H. S., Ed.; American Scientific Publishers: Valencia, CA, 2003.
- (17) Turro, N. J.; Weed, G. C. *J. Am. Chem. Soc.* **1983**, *105*, 1861.
- (18) Scaiano, J. C.; Joannovic, S. V.; Morris, D. G. *J. Photochem. Photobiol. A* **1998**, *113*, 197.
- (19) Periasamy, N.; Linschitz, H. *Chem. Phys. Lett.* **1979**, *64*, 281.
- (20) Shafirovich, V. Y.; Batova, E. E.; Levin, P. P. *J. Phys. Chem. A* **1993**, *97*, 4877.
- (21) Steiner, U. E.; Haas, W. *J. Phys. Chem.* **1991**, *95*, 1880.
- (22) Mori, Y.; Sakaguchi, Y.; Hayashi, H. *J. Phys. Chem. A* **2002**, *106*, 4453.
- (23) Mori, Y.; Sakaguchi, Y.; Hayashi, H. *J. Phys. Chem. A* **2000**, *104*, 4896.
- (24) Igarashi, M.; Sakaguchi, Y.; Hayashi, H. *Chem. Phys. Lett.* **1995**, *243*, 545.
- (25) Aich, S.; Basu, S. *Chem. Phys. Lett.* **1997**, *281*, 247.
- (26) Sakaguchi, Y.; Hayashi, H. *J. Phys. Chem. A* **1997**, *101*, 549.
- (27) Ali, S. S.; Maeda, K.; Murai, H.; Azumi, T. *Chem. Phys. Lett.* **1997**, *267*, 520.
- (28) Levin, P. P.; Raghavan, P. K. N.; Kuzmin, V. A. *Chem. Phys. Lett.* **1990**, *167*, 67.
- (29) Shimada, E.; Nagano, M.; Iwahashi, M.; Mori, Y.; Sakaguchi, Y.; Hayashi, H. *J. Phys. Chem. A* **2001**, *105*, 2997.
- (30) Steiner, U. *Chem. Phys. Lett.* **1980**, *74*, 108.
- (31) Mori, Y.; Sakaguchi, Y.; Hayashi, H. *Chem. Phys. Lett.* **1998**, *286*, 446.
- (32) Ulrich, T.; Steiner, U. E.; Foell, R. E. *J. Phys. Chem.* **1983**, *87*, 1873.
- (33) Dey, D.; Bose, A.; Chakraborty, M.; Basu, S. *J. Phys. Chem. A* **2007**, *111*, 878.
- (34) Sugimori, T.; Masuda, H.; Ohata, N.; Koiwai, K.; Odani, A.; Yanmauchi, O. *Inorg. Chem.* **1997**, *36*, 576.
- (35) Waring, M. J. *J. Mol. Biol.* **1965**, *13*, 269.
- (36) Luisi, P. L.; Giomini, M.; Pileni, M. P.; Robinson, B. H. *Biochim. Biophys. Acta* **1988**, *947*, 209.
- (37) Imre, V. E.; Luisi, P. L. *Biochem. Biophys. Res. Commun.* **1982**, *107*, 538.
- (38) Aich, S.; Basu, S. *J. Chem. Soc., Faraday Trans.* **1995**, *91*, 1593.
- (39) Dutta Choudhury, S.; Basu, S. *J. Phys. Chem. B* **2006**, *110*, 8850.
- (40) Aubert, C.; Mathis, P.; Eker, A. P. M.; Brettel, K. *Biochemistry* **1999**, *38*, 5423.
- (41) Dey, D.; Bose, A.; Pramanik, N.; Basu, S. *J. Phys. Chem. A* **2008**, *112*, 3943.
- (42) Wakasa, M.; Hayashi, H.; Mikami, Y.; Takeda, T. *J. Phys. Chem.* **1995**, *99*, 13181.
- (43) Ma, J.; Lin, W.; Wang, W.; Han, Z.; Yao, S.; Lin, N. *J. Photochem. Photobiol. B* **2000**, *57*, 76.
- (44) Wagenknecht, H.-A.; Rajske, S. R.; Pascaly, M.; Stemp, E. D. A.; Barton, J. K. *J. Am. Chem. Soc.* **2001**, *123*, 4400.
- (45) Steenken, S.; Jovanovic, S. V. *J. Am. Chem. Soc.* **1997**, *119*, 617.
- (46) Wagenknecht, H.-A.; Stemp, E. D. A.; Barton, J. K. *Biochemistry* **2000**, *39*, 5483.

JP810778B